APPLIED AND ENVIRONMENTAL MICROBIOLOGY, Aug. 1990, p. 2327–2340
0099-2240/90/082327-14$02.00/0

Vol. 56, No. 8

Spectral Irradiance and Distribution of Pigments in a Highly Layered Marine Microbial Mat

BEVERLY K. PIERSON,* VICKI M. SANDS,† AND JUDITH L. FREDERICK‡
Biology Department, University of Puget Sound, Tacoma, Washington 98416

Received 31 January 1990/Accepted 15 May 1990

The spectral irradiance from 400 to 1,100 nm was measured with depth in the intertidal sand mats at Great Sippewissett Salt Marsh, Mass. These mats contained at least four distinct layers, composed of cyanobacteria, purple sulfur bacteria containing bacteriochlorophyll *a* (Bchl *a*), purple sulfur bacteria containing Bchl *b*, and green sulfur bacteria. Spectral irradiance was measured directly by layering sections of mat on a cosine receptor. Irradiance was also approximated by using a calibrated fiber-optic tip. With the tip, irradiance measurements could be obtained at depth intervals less than 250 μm. The irradiance spectra were correlated qualitatively and quantitatively with the distribution of the diverse chlorophyll pigments in this mat and were compared with spectra recorded in plain sand lacking pigmented phototrophs. We found that the shorter wavelengths (400 to 550 nm) were strongly attenuated in the top 2 mm of the mat. The longer wavelengths (red and near infrared) penetrated to much greater depths, where they were attenuated by Bchl *a*, *b*, and *c*-containing anoxygenic phototrophic bacteria. The specific attenuation bands in the irradiance spectra correlated with the specific in vivo absorption bands of the Bchl-protein complexes in the bacteria. We concluded that the pigments in the phototrophs had a profound affect on the light environment within the mat. It seems likely that the diverse Bchl-protein complexes found in the anoxygenic phototrophs evolved in dense mat environments as a result of competition for light.

The light environment within microbial mats is influenced by several biological and abiological factors. The type of mat fabric, inorganic matrix, pigments within microorganisms, extracellular pigments, living and dead cells, microbial mucilage, and overlying water can influence the quantity and quality of light present. For mats composed of largely phototrophic microorganisms, understanding the nature of the light environment is important to gain an understanding of the limiting factors within this environment. In highly layered mats of phototrophs, the light-dependent metabolic activities may be significantly affected by the changing light environments within the layers. The highly pigmented phototrophs themselves greatly alter this aspect of the environment.

Various attempts have been made to analyze the light environment in microbial mats and marine sediments, some with greater sensitivity and resolution than others (3, 4, 6–10, 16, 18, 19, 21, 22). Analyses of pigments in microbial mat layers suggest how the qualitative light environment may be altered. Such analyses have been conducted by using high-resolution visible absorption spectroscopy of homogenized mat layers (16) or photoacoustic spectroscopy of intact mat layers (18). However, only direct measurement of the spectral distribution of radiation within the mat accurately describes the light environment surrounding the microorganisms. Total irradiance in sediments or mat environments has been measured by burying a sensor in the mat or layering the mats upon a sensor (16, 21, 22). Spectroradiometric measurements at moderate resolution have been made in a similar manner in soil (1, 4, 23). Attenuation of broadband monochromatic light has been used to approximate the light environment within sediments (3, 4). Jørgensen et al. (6–10) have developed a fiber-optic microprobe which could be inserted into a piece of mat. When coupled with a diode detector and illuminated from above through a continuous-interference filter, this microprobe can measure the selective attenuation of the various illuminating wavelengths with high depth resolution but limited wavelength resolution in the mat.

Our primary objective in studying microbial mats has been to gain a better understanding of the distribution and role of anoxygenic phototrophs in highly layered mat communities (14, 16). Of major importance to this objective is knowledge of the actual light environment experienced by these microorganisms in situ. We therefore developed a system that would permit the direct measurement of spectral irradiance at different depths in mats under ambient conditions in situ. A second objective of our study was to determine how the light penetration in microbial mats was affected by the pigmentation of the microorganisms within the mat.

In this communication we describe the use of a battery-operated spectroradiometer equipped with a remote cosine sensor to measure downward spectral irradiance in layered microbial mats under natural conditions in the field. This system required slicing and layering the mat on the sensor. We also describe the development of a fiber-optic milliprobe which, when used with the spectroradiometer, permitted measurements approximating downward spectral irradiance at much smaller depth intervals (100 μm) than could be obtained with the remote cosine sensor (1,000 μm). The fiber-optic tip could be pushed up through the mat, thereby avoiding slicing and layering the mat. We have compared the spectral irradiance in mats with the distribution of pigments within the mats. Our analytical system has been used to obtain spectral irradiance data from different types of mats. Here we report the data obtained from the highly layered marine mats of Great Sippewissett Salt Marsh, Mass.

* Corresponding author.
† Present address: Health Sciences Center of Oregon, Portland, OR 97201.
‡ Present address: Department of Biological Sciences, Yale University, New Haven, CT 06511-7444.

The mats at Great Sippewissett (14, 16) consist of an upper gold layer of diatoms and cyanobacteria, a green layer of primarily filamentous cyanobacteria, a pink layer of purple sulfur bacteria containing bacteriochlorophyll *a* (Bchl *a*) (primarily *Thiocapsa* and *Chromatium* species), a peach layer of purple sulfur bacteria containing Bchl *b* (*Thiocapsa pfennigii*), and an olive layer of green sulfur bacteria containing Bchl *c* (*Prosthecochloris aestuarii*). Owing to the large number of different layers containing such a large variety of pigments, this mat was particularly well suited to a study of the specific effects of pigment-protein complexes on the light environment.

MATERIALS AND METHODS

Spectral irradiance. Most of the measurements reported here were obtained in July and August 1986 and 1987. Spectra were recorded by using normal incident solar radiation at the field site where mat samples were collected.

Downward spectral irradiance was measured with a battery-powered portable spectroradiometer (LI-1800; Li-Cor, Inc., Lincoln, Nebr.) operated with a portable LCD terminal (LI-1800-01). An irradiance sensor, the remote cosine receptor (LI-1800-11), was connected to the spectroradiometer with a quartz fiber-optic cable (LI-1800-10). The sensor was buried directly in the mat at different depths as previously described (16). Alternatively, cores (1.0 to 1.5 cm in diameter) were taken from the mat and centered over the 7.0-mm-diameter sensor. When slicing the mat to take consecutive measurements with depth through a core, the thinnest slices we could obtain were 500 μm. Most mats could not be sliced any finer than 1,000 μm. A fiber-optic milliprobe sensor system was therefore developed to increase the depth resolution for measurements within mats and to facilitate making measurements without having to slice the mat into sections.

The sensors were blunt or tapered fiber-optic tips (0.2 to 0.8 mm in diameter) pulled from 3.0-mm-diameter glass fiber image conduit (3050 fused 50-μm-diameter glass fibers; Edmund Scientific Co., Barrington, N.J.). Tips were 3 to 4 cm in length and were painted black along the sides to prevent the entry of extraneous light. The tips were very strong and penetrated most mats easily with no breakage. The base of each tip was fitted flush to the end of the quartz fiber-optic receptor cable, which connected directly to the spectroradiometer. For some measurements a flexible glass fiber-optic light guide (Edmund Scientific) was used between the tip and the quartz fiber-optic cable to increase flexibility. This glass fiber-optic extender resulted in an even loss of irradiance across the spectrum.

The tip was mounted in a custom-built micrometer table of solid aluminum. The table consisted of a platform (19 by 13.5 cm) mounted on legs (10 cm long) with leg extenders to increase the height to 25 cm. A small hole through the platform permitted the insertion of the fiber-optic tip into the base of a mat core. The core was taken with a glass corer (height, 1 cm; inner diameter, 2 cm). The core within the corer was mounted in a blackened cup (core chamber) with a cover that permitted exposure of only the surface of the core to incident solar radiation. Mat samples less than 1 cm high were positioned on agar plugs of appropriate thickness.

The core chamber was fitted into the platform so that the core was centered over the hole in the platform. The tip was mounted in a chuck and centered with three set screws. The chuck was attached to a horizontal arm connected directly to a vertically oriented micrometer with a vernier scale. By simply rotating the vernier, the tip could be advanced up through the mat from base to surface in the desired increments. Most often spectra were recorded at increments of 250, 500, or 1,000 μm. Increments as small as 100 μm were used. Incident solar spectra were recorded with the tip just emerging from the surface of the mat.

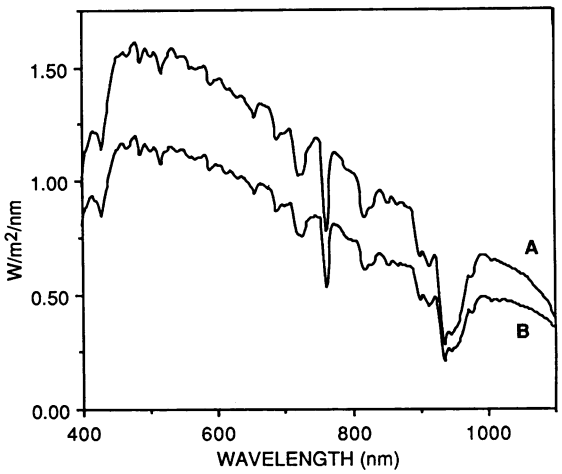

FIG. 1. Spectral irradiance of sun and sky obtained with a cosine receptor (A) and a fiber-optic tip (B) recorded at noon on 7 July under a clear sky.

Spectral irradiance was measured from 400 to 1,100 nm at 2-nm intervals with the remote cosine receptor or was approximated with a fiber-optic tip over the same range (see below). Either single spectra or multiple spectra (which were then averaged) were recorded. Recording irradiance at 2-nm intervals provided excellent wavelength resolution for spectral irradiance. Using 1-nm intervals consumed too much memory for field work and did not significantly increase resolution for our objectives.

The fiber-optic sensor tips were spectrally calibrated to approximate irradiance sensors by using the Optical Radiation Calibrator (LI-1800-02; Li-Cor). The calibrator uses a 200-W quartz tungsten halogen lamp. The calibration spectrum for each tip was stored in the LI-1800 memory banks, and all collected spectra were immediately corrected with the calibration file for the appropriate tip. When tested with a point source, the percent ideal cosine response of a tip was 94 to 95% at a 10° half angle, 78 to 79% at a 20° half angle, 54 to 56% at a 30° half angle, 28 to 32% at a 40° half angle, 10 to 12% at a 50° half angle, and less than 10% at half angles greater than 50°. The percent ideal cosine response of the tip varied by less than 10% as a function of wavelength over the range from 400 to 1,100 nm. Therefore, the optical properties of the tips were not ideal. At high solar angles, achieved midday in May through August, the measurements recorded with these tips only approximated true spectral irradiance. Figure 1 compares solar spectra recorded with a calibrated tip and with the calibrated remote cosine receptor. It is clear that these solar measurements with the tip were not the same as spectral irradiance measured with the cosine receptor. The values obtained with the tip ranged from 70 to 76% of the values obtained with the cosine receptor. Because the optical properties within mats are poorly understood and are likely to vary in different mats, we relied on empirical evidence to determine whether the tip response was similar to that of the cosine receptor in situ. Figure 2 compares the spectral irradiance recorded with the remote cosine receptor

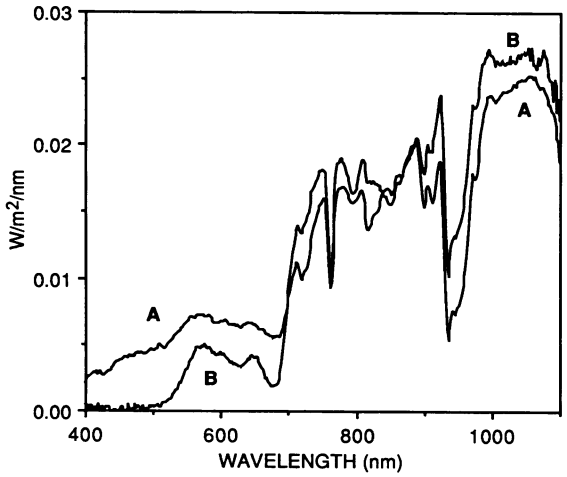

FIG. 2. Spectral irradiance recorded at a depth of 2.5 mm in a mat from Great Sippewissett Salt Marsh. Spectra were recorded directly beneath the green cyanobacterial layer on two adjacent mat samples. (A) The sample was placed over the calibrated remote cosine receptor. (B) The sample was penetrated with a calibrated fiber-optic tip.

and a fiber-optic tip in the optically diffuse environment of the mat. Spectra were recorded in similar mat cores at similar depths. Although not ideal, the calibrated tip obtained measurements similar to those obtained with the remote cosine receptor within the mat. We are continuing to work to improve the collecting characteristics of the tips without increasing their size or decreasing their penetrability into the mat fabric. The data presented here for fiber-optic tips will be reported as spectral irradiance with the caution that our numbers are not identical with spectral irradiance values obtained with a cosine receptor and only approximate the downward irradiance. We believe that the numbers are close enough, however, to be useful indicators of the downward irradiance reaching different layers of phototrophs within the mat. Numbers obtained with the tips will always be noted as approximate spectral irradiance, to distinguish them from true or actual spectral irradiance measured with the remote cosine receptor. No attempt was made to calculate true spectral irradiance from measurements made with the tips.

Upwelling irradiance was approximated by mounting the tip in a Leitz Wetzlar micromanipulator and inserting the tip from the surface downward into the mat at an angle of 15° from the vertical.

Pigment analysis. Methods for determining in vivo absorption spectra of sonicated cells in buffer and for quantifying pigments in methanol extracts of mat samples were previously reported (16).

RESULTS

Spectral composition of downward irradiance through colored layers of mat. The spectral composition of the downward irradiance through the mat was altered as it passed through the colored layers of mat. A series of spectra of downward irradiance recorded immediately beneath each colored layer in a core mounted above the remote cosine receptor revealed these alterations over the range from 300 to 1,100 nm (Fig. 3) (17). The solar signature (Fig. 3a) at the surface of the mat was still detectable beneath the top gold layer of diatoms and cyanobacteria (Fig. 3b) at wavelengths greater than 700 nm. Dramatic attenuation of the incident solar radiation was seen below 700 nm, with specific troughs at 670 to 680 nm due to chlorophyll *a* (Chl *a*), 620 to 630 nm due to phycocyanin, and 580 to 590 nm due to phycoerythin. A much broader attenuation occurred from 350 to 500 nm due to absorption by carotenoids, chlorophylls (Soret peaks), and other pigments. Beneath the green layer in the mat (primarily cyanobacteria) at a depth of about 3 mm (Fig. 3c), all radiation below 500 nm had fallen below detection levels and little radiation remained at 670 nm. The solar signature was still recognizable in the near infrared (NIR), but a trough was detected between 800 and 860 nm due to absorption by Bchl *a*. Beneath the pink layer (primarily purple sulfur bacteria) the solar signature was no longer recognizable (Fig. 3d). The only wavelengths transmitted to this depth were those in a broad peak from 700 to 790 nm, two small peaks (810 to 830 nm and 910 to 930 nm), and the wavelengths beyond 950 nm. A distinct trough was seen in the NIR near 1,020 nm; this was due to Bchl *b*. Troughs at 794 and 843 nm were due to Bchl *a*. Below the peach layer (Fig. 3e), no significant radiation was detected. This layer was composed of purple sulfur bacteria containing Bchl *b* and green sulfur bacteria containing Bchl *c*.

Correlation of spectroradiometric transmission through individual mat layers with absorption spectra of pigment-protein complexes isolated from the layers. To study the transmission properties of each colored layer of mat for unattenuated solar radiation, disks of each colored layer (1 to 2 mm thick) were cut from a core and transmission spectra were recorded through each disk of sediment. The cells were then washed from the sand grains, and a membrane fraction was prepared for in vivo absorption spectroscopy of the pigment-protein complexes. The absorption spectra obtained were superimposed on the transmission spectra taken through the intact sample (Fig. 4) to determine the relationship between the absorption maxima of the pigments and the transmission minima of the sediment sample. In Fig. 4a (gold layer) the major absorption maximum at 673 nm correlated with the sharp trough at 670 nm. Even the Chl *a* Soret peak at 435 nm can be recognized in the massive attenuation in the transmission spectrum. A similar pattern was seen for the green layer (Fig. 4b), with an additional correlation of strong absorbance maxima at 794 and 843 nm with transmission minima at these wavelengths due to small amounts of Bchl *a* in this mat layer. The spectrum through the pink layer (Fig. 4c), with very reduced Chl *a* relative to Bchl *a*, revealed the correlation between the 590-nm Bchl *a* peak and a transmission trough. The relatively small amount of Chl *a* does not make a distinct trough at 670 nm but, rather, broadens the existing solar trough at 690 nm. As in the gold and green layers, the high level of absorption by carotenoids and Soret peaks of chlorophylls resulted in a large attenuation of radiation transmitted below 600 nm through the pink layer (Fig. 4c). The transmission of spectral irradiance through the pink layer differed dramatically from the transmission through the green and gold layers due to the massive NIR attenuation, caused by Bchl *a*, that is as great as that below 600 nm due to the presence of carotenoids. The broad absorption near 1,015 nm from Bchl *b* was detected as a trough between 1,000 and 1,030 nm.

The less intense absorption by carotenoids in the peach layer (Fig. 4d) was apparent in the greater transmission in the region below 600 nm. The distinct trough at 590 nm corresponds to the absorbance of Bchl *b* (and Bchl *a*). The absorption by Bchl *c* at 743 to 747 nm was seen as a broadening of the solar trough at 720 nm with attenuation of

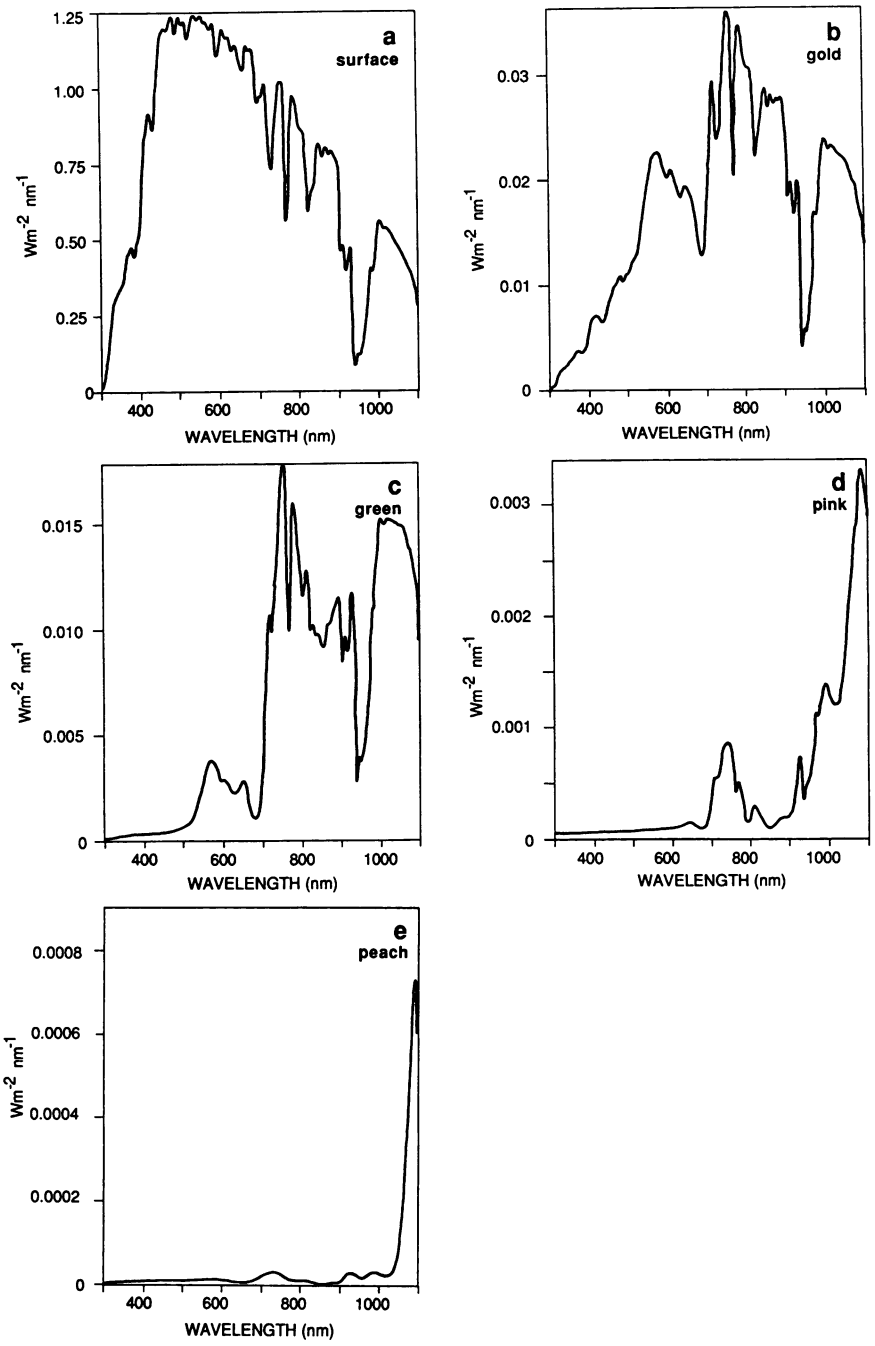

FIG. 3. Spectral irradiance recorded at the surface and beneath each colored layer from the surface to the base of a highly layered mat at Great Sippewissett Salt Marsh (17). Spectra were recorded by using a calibrated cosine receptor. (a) Surface of mat (incident solar spectrum); (b) spectral irradiance beneath the surface gold layer of diatoms and cyanobacteria; (c) spectral irradiance beneath the surface gold layer and the green layer of cyanobacteria; (d) spectral irradiance beneath the gold layer, green layer, and pink layer of purple sulfur bacteria; (e) spectral irradiance beneath gold, green, and pink layers and the peach layer of purple sulfur bacteria.

transmission from 730 to 750 nm. The absorbance of small amounts of Bchl *a* was seen in troughs at 790 and 820 to 850 nm. The largest distinct trough in the transmitted radiation, however, was at 1015 to 1020 nm, corresponding to the major absorption band of Bchl *b*.

The transmission characteristics of the olive layer (Fig. 4e) differed significantly from those of the pink, green, and gold layers and were similar to those of the peach layer in having greater transmission in the range from 500 to 600 nm due to reduced absorption by carotenoids. The olive layer had very little Bchl *a*, as seen by the persistence of the narrow solar trough at 820 nm, not broadened by the 840-nm Bchl *a* absorbance seen in Fig. 4c and d. Considerable Bchl *b* was present in the absorption spectrum of the olive layer, and this was revealed by the deep trough near 1,015 nm in the transmission spectrum. The presence of a relatively higher

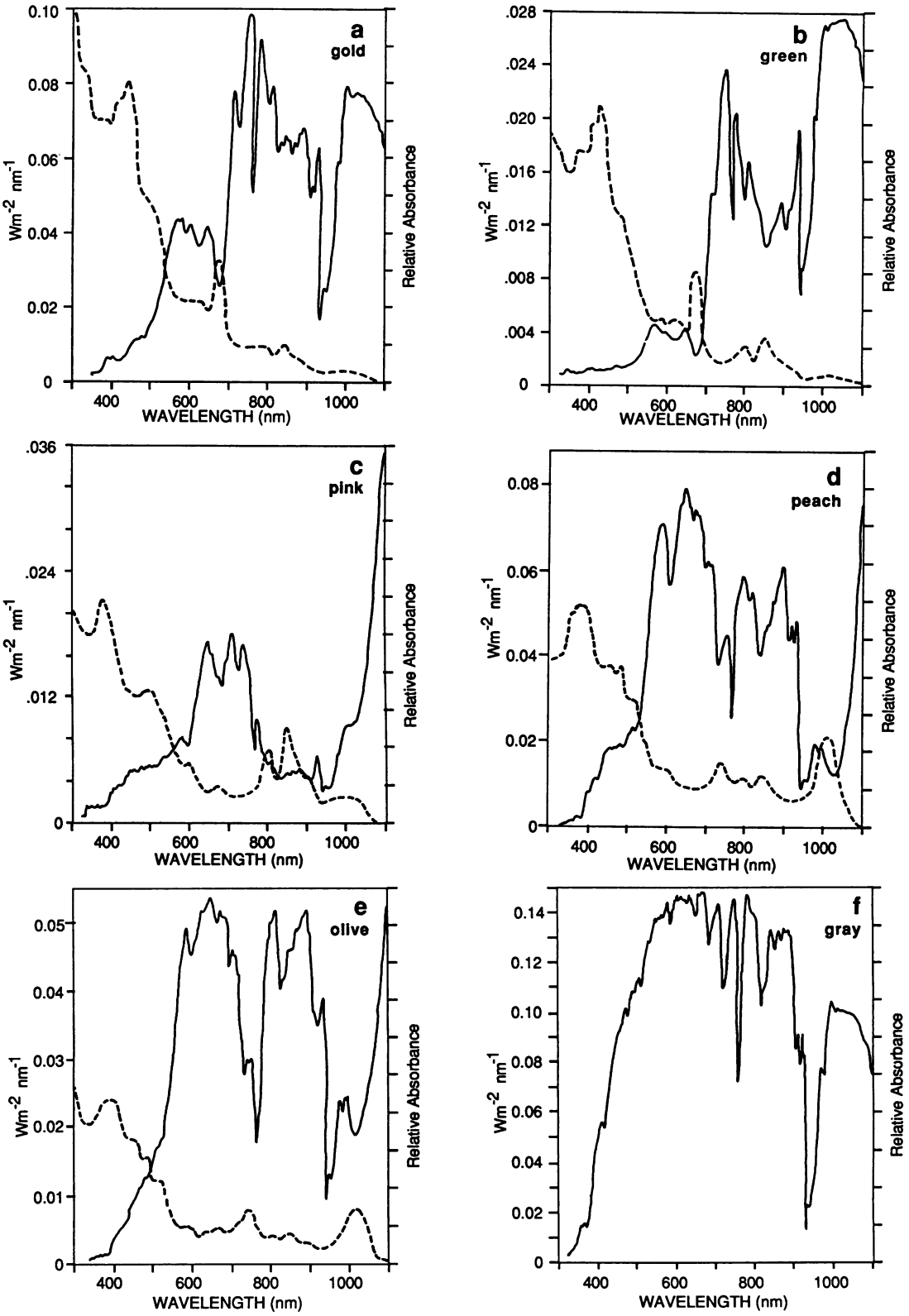

FIG. 4. Spectral irradiance transmitted by each isolated colored layer of mat (——) with accompanying absorption spectrum of pigment-protein complexes isolated from the same layer of mat (– – –). (a) Gold surface layer of cyanobacteria and diatoms; (b) green layer of cyanobacteria; (c) pink layer of purple sulfur bacteria containing Bchl *a*; (d) peach layer of purple sulfur bacteria containing Bchl *b*; (e) olive layer of green sulfur bacteria and Bchl *b*-containing purple sulfur bacteria; (f) gray sand layer beneath mat. Spectral irradiances were measured with a calibrated cosine receptor. Pigment-protein complexes were prepared from cells sonicated in buffer.

density of Bchl *c* was reflected in the deep attenuation near 740 nm.

A transmission spectrum taken through a 1-mm-thick slice of gray sand below the olive layer was remarkably similar to the solar spectrum and revealed no chlorophyll pigments (Fig. 4f).

Attenuation of radiation with depth in the mat relative to pigment concentration. The attenuation of radiation in the spectral region absorbed by the pigment-protein complexes in the microorganisms within the mat was compared with the quantitative distribution of the chlorophylls in the mat (Fig. 5). A mat core was placed on the detector surface, and spectra were recorded from the base of the mat to the top in 1-mm increments. As each 1 mm of mat was sliced from the base of the core, pigments were extracted in methanol and quantified.

The concentration of each chlorophyll (in micrograms per cubic millimeter of sediment) is plotted at 1-mm depth increments in Fig. 5. Accompanying the depth distribution for each chlorophyll is the depth distribution for the in situ attenuation at its absorption maximum in the mats. The relative attenuation at the absorption maximum for each pigment was calculated as a ratio of the irradiance at a nonabsorbed reference wavelength to the irradiance at the absorption maximum. The nonabsorbed wavelength was arbitrarily chosen within 40 nm of the absorption maximum of the pigment. In selecting reference wavelengths, it was necessary to avoid wavelengths absorbed by any pigments as well as wavelengths occurring in steeply changing parts of the residual solar spectrum. At depths where there was equal attenuation at both wavelengths, the ratio was close to 1.0. At depths where the pigment absorbed strongly, the irradiance in the mat at the absorption maximum was much lower than at the nonabsorbed wavelength and the ratio became greater than 1.0. In general, maximum attenuation for each chlorophyll measured by spectroradiometry occurred in the region of its maximal concentration determined in pigment extracts. The correlations were very positive in the upper 4 to 5 mm of mat, where irradiances were relatively high. Below this depth, however, where irradiances became very low and noise levels were greater, the correlations were less precise.

The attenuation ratio for Chl *a* (I_{700}/I_{676}) was at its highest value (much greater than 1.0) in the top 4 mm of the mat, where the concentration of Chl *a* was highest (Fig. 5). The attenuation ratio fell to values near 1.0 as the concentration of Chl *a* fell to 0. The attenuation ratio for Bchl *a* (I_{880}/I_{844}) was highest between 3 and 6 mm, where the concentration of Bchl *a* was highest. At the very low irradiances found deep in the mat it was more difficult to calculate reliable attenuation factors for Bchl *b* and Bchl *c*. The maximum attenuation ratio for Bchl *b* ($I_{1,050}/I_{1,016}$) was found between 5 and 7 mm, where the concentration of Bchl *b* was high. A significant increase in irradiance was detected at 1,016 nm, however, before Bchl *b* was detected in pigment extracts. The attenuation ratios for Bchl *c* were particularly difficult to determine because of the very low irradiances at the base of the mat and because there was no satisfactory reference wavelength within 40 nm of the absorption maximum at 744 nm. The reference wavelengths from 700 to 740 nm and from 750 to 800 nm fell on steep solar troughs and were not easily used. The reference wavelength of 780 nm was chosen because it was not on the steepest slopes. Unfortunately, Bchl *a* has a strong absorption maximum at 790 nm and consequently absorbs significantly at 780 nm. This was seen in a decrease in the attenuation ratio to values much less than 1.0 from 4 to 6 mm in the mat, where Bchl *a* was present. The attenuation by Bchl *c* at 744 nm relative to 780 nm was seen as the sharp increase in the attenuation ratio at the 6- to 8-mm depth, where Bchl *c* was concentrated.

Spectral distribution of radiation in the mat measured with a fiber-optic milliprobe. The downward spectral irradiance was measured in a core of the mat by using the fiber-optic milliprobe. Whereas the numbers were not a precise measure of irradiance, they were reasonable approximations. The spectral irradiance was recorded at the surface of the mat (Fig. 6a) and at 500-μm intervals throughout the mat to a depth of 4.5 mm. The impact of the pigments in the mat layers on the spectral irradiance collected with the fiber-optic milliprobe is readily seen in these spectra. No radiation below 500 nm was detected at a depth of 2.0 mm, and little was detected at 1.5 mm. The large absorption by Chl *a* was evident from the deep attenuation trough at 670 nm in the first 0.5 mm. Evidence for some attenuation at 790 and 840 nm (due to Bchl *a*) can be seen in the top 2 mm, but the troughs are most distinct at 2.5 and 3.0 mm, where the pink layer of purple sulfur bacteria occurred in this sample. Below this depth the attenuation trough due to absorption by Bchl *b* (around 1,016 nm) in the purple sulfur bacterium *Thiocapsa pfennigii* forming the peach layer became prominent. The wavelength resolution of the spectral composition of the radiation within the mat with depth was as sensitive with the tip as with the remote cosine receptor (Fig. 3).

Penetration of downward irradiance in mat and sand and analysis of upward irradiance. The mats at Great Sippewissett have developed in a wet sand matrix (14). We compared the optical properties of the mat itself with those of the inorganic sand matrix by preparing plain wet sand cores from the sand found adjacent to the mat areas. We were particularly interested in seeing the impact of the microorganisms on the penetration of light in the sand.

The difference in penetration of downward irradiance in mat and plain wet sand is illustrated in Fig. 7, which shows the percentage of surface irradiance at the wavelengths where pigments absorb maximally. It can clearly be seen that the penetration is much greater in plain wet sand than in the mat where pigments absorb the radiation strongly at these wavelengths. Both in the mat and in plain sand, the longer wavelengths penetrated the furthest.

Table 1 compares the depths at which wavelengths selected at 100-nm intervals penetrate to 1.0 and 0.1% of their surface values. Shorter wavelengths (less than 500 nm) are attenuated to 0.1% of surface values at a depth of about 2.0 mm in the mat but penetrate to 6.8 mm in sand. The longest wavelengths (1,000 to 1,050 nm) penetrate to about 6.0 mm in the mat as opposed to 9.0 mm in plain sand. The difference in depth of penetration in mat versus sand across the entire spectrum ranges from 1.6 to nearly 4 mm, illustrating the significant impact of the presence of microorganisms on the penetration of radiation in sediments.

Plain sand and even mats can provide a highly scattering optical environment in which reflected and backscattered radiation could influence the total irradiance impinging on any point in the matrix.

In Table 2 we compared the upward irradiance (expressed as a percentage of the downward irradiance) at different depths in plain sand and mat. The spectral irradiances were measured at the wavelengths absorbed by the major pigments in the mat (370, 436, 676, 748, 844, and 1,016 nm). The integrated irradiances from 350 to 1,100 nm in sand and in mat are compared in the last two columns of Table 2. At all wavelengths and all depths, the upward irradiance in the mat

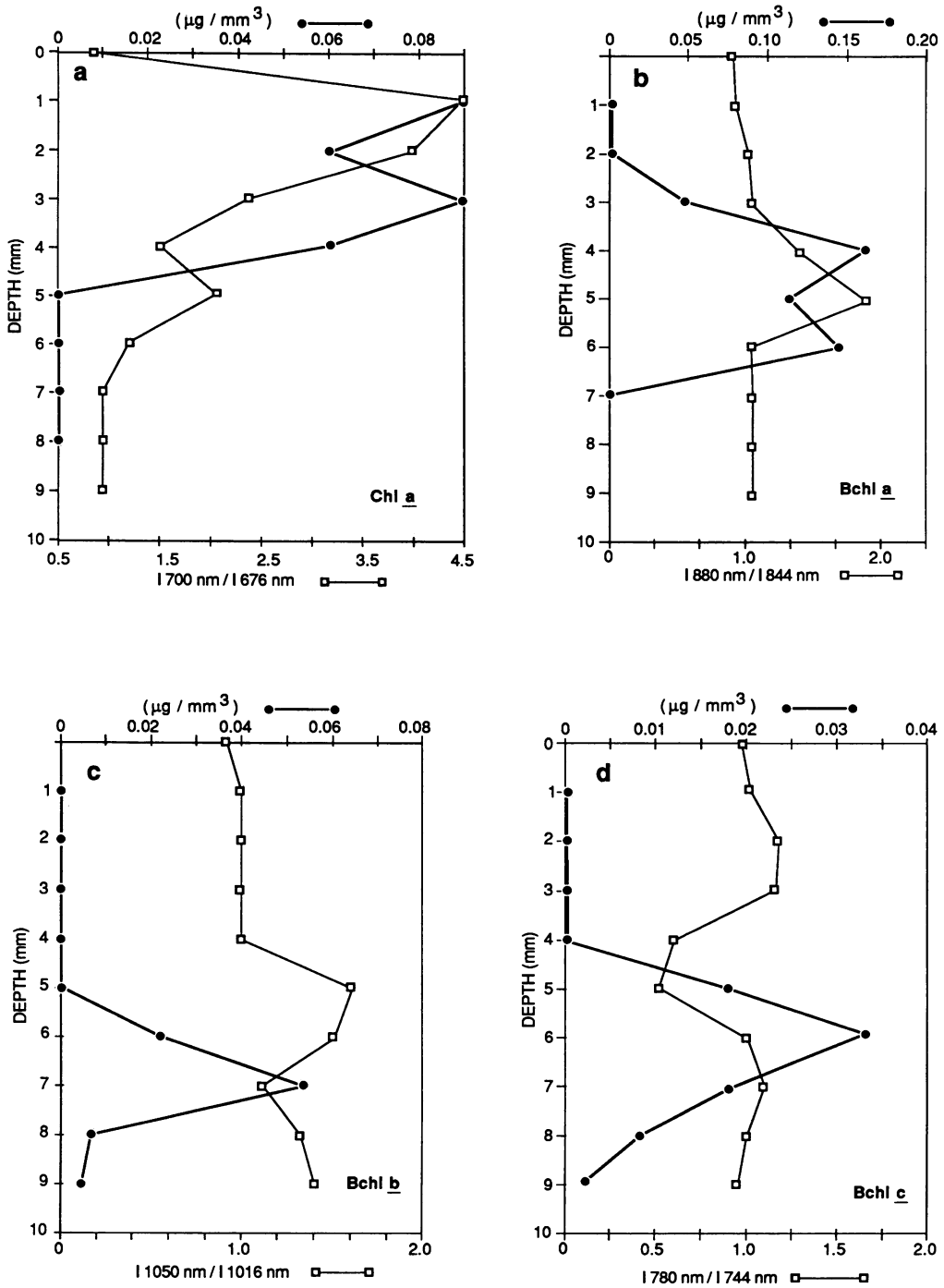

FIG. 5. Attenuation of radiation absorbed by specific chlorophylls with depth plotted with the quantitative distribution of chlorophylls with depth. The attenuation of each chlorophyll with depth was calculated from the ratio of the irradiance at a wavelength not absorbed by the pigment to the irradiance at the absorption maximum of the pigment in situ. At depths with little or no attenuation by the pigment, these ratios were close to 1.0. At depths where the pigment absorbed strongly and hence produced strong attenuation of irradiance at its absorption maximum, the ratio was greater than 1.0. The concentration of pigment (in micrograms per cubic millimeter of sediment) was calculated from methanol extracts of each 1-mm segment of mat.

was significantly reduced over that in plain wet sand. In both sand and mat the percentage of upward irradiance at a given depth was higher at the longer wavelengths. The percentage of upward irradiance also decreased with depth (very dramatically in the first 0.5 mm). At the very surface of the plain sand the upward irradiance nearly equaled the downward irradiance at the longest wavelengths. Upward irradiance at the surface of the mat was 70% of the downward irradiance at 1,016 nm. These exceptionally high upward irradiances obtained at the surface of the sand and mat were probably

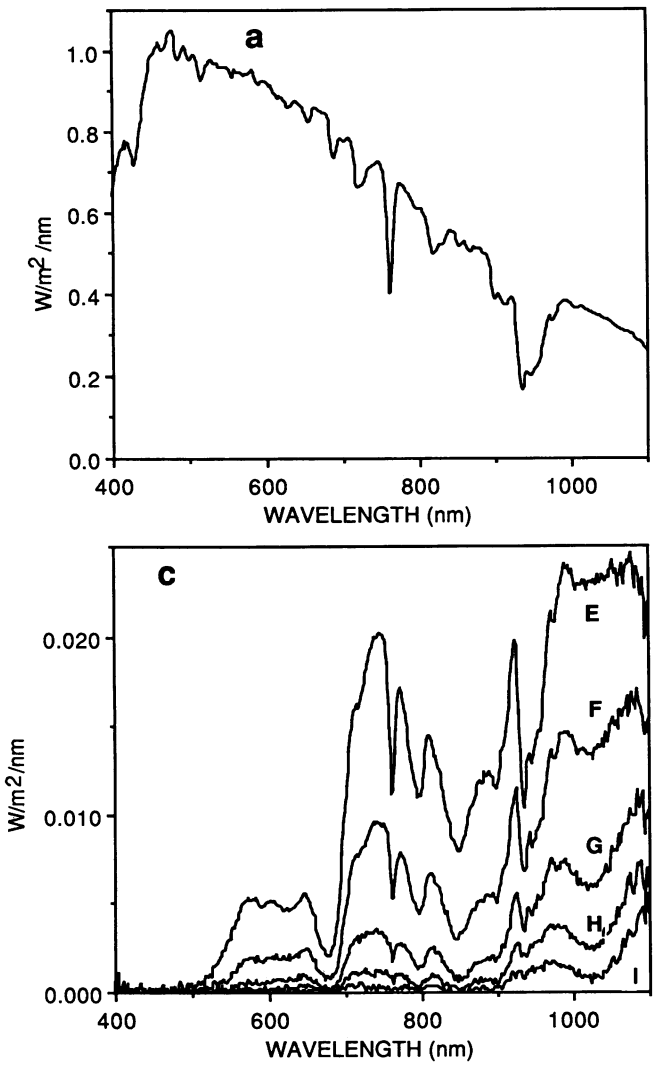

distorted by the poor collecting properties of the fiber-optic tip at the lower sun angles at which these spectra were recorded. At a depth of 0.5 mm, however, the upward irradiance had fallen to less than 10% of the downward irradiance in the mat at all wavelengths below 900 nm. Only at 1,016 nm did the upward irradiance constitute more than 10% of the downward irradiance at depths of 0.5 mm or more. This high level of upward irradiance in the NIR fell to less than 10% at depths greater than 2 mm.

Total downward irradiance available for different phototrophs with depth. The spectral irradiances over 100-nm intervals were integrated and plotted as bar graphs (Fig. 8) to indicate the total irradiance available over 100-nm ranges at 1-mm depth intervals. The integration of the data over these arbitrary ranges is particularly useful for estimating the total downward irradiance available to particular phototrophs at each depth. Since the pigments in vivo have fairly broad absorption bands, the irradiance at the absorption maximum for a pigment is too narrow an indication of what is available for actual use by the organism. All of the organisms absorb strongly in the region from 400 to 500 nm and somewhat less strongly in the region from 500 to 600 nm owing to carotenoids and the Soret peaks of the chlorophylls. In the red and NIR parts of the spectrum, the absorption by each group

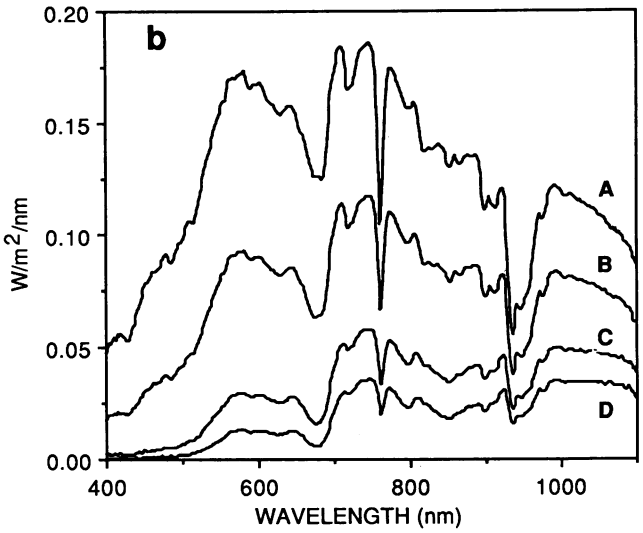

FIG. 6. Depth profile of spectral irradiance approximated with a fiber-optic tip pushed through the mat in 0.5-mm increments. (a) Solar spectral irradiance at the surface of the mat; (b) spectral irradiance from 0.5 to 2.0 mm; (c) spectral irradiance from 2.5 to 4.5 mm.

of organisms is confined to one discrete region of the spectrum. The cyanobacteria absorb strongly from 600 to 700 nm due to phycocyanin and Chl *a*. The green sulfur bacteria absorb in the range of 700 to 800 nm owing to Bchl *c*, Bchl *d*, or Bchl *e*. The purple sulfur bacteria containing Bchl *a* absorb strongly with two or more absorption maxima from 800 to 900 nm. The purple sulfur bacteria with Bchl *b* absorb primarily at 1,000 to 1,100 nm with some absorption in the 800- to 900-nm range. In this particular mat no organisms absorb from 900 to 1,000 nm. By regarding the irradiance in this way we draw attention to what is available at each depth in the mat for all potential inhabitants from each group of phototrophs rather than narrowing our perspective to just those organisms that are present in this particular mat. At the surface of the mat (Fig. 8A), the irradiance exceeded 300 μmol m^{-2} s^{-1} in each of the spectral ranges 500 to 600 nm, 600 to 700 nm, and 700 to 800 nm. An

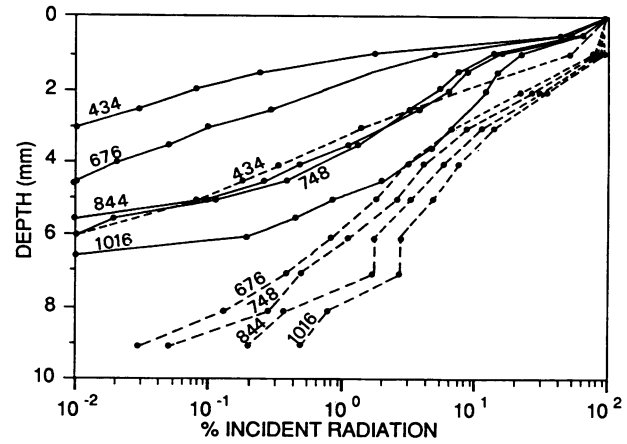

FIG. 7. Percent incident (surface) irradiance occurring at 0.5-mm depth increments in the mat (——) and in plain wet sand (– – –) determined at the absorption maxima of the various pigments.

TABLE 1. Depth of penetration of downward irradiance to 1.0 and 0.1% of surface values

Wavelength (nm)	Depth (mm)			
	1.0% of surface value		0.1% of surface value	
	Sand	Mat	Sand	Mat
400	2.8	1.2	3.5	1.7
500	4.0	1.3	6.8	2.2
600	5.3	2.2	7.9	3.8
700	6.0	2.8	8.2	4.8
800	6.8	3.6	8.9	5.2
900	7.3	4.2	8.9	5.5
1,000	7.0	5.0	8.9	5.9
1,050	7.5	5.3	8.9	6.5

irradiance of 280 μmol m^{-2} s^{-1} was found from 400 to 500 nm and from 800 to 900 nm. The lowest irradiances (200 to 225 μmol m^{-2} s^{-1}) were found in the 900- to 1,000-nm and 1,000- to 1,100-nm ranges. Within the first 1 mm of the mat (Fig. 8B) the irradiances below 700 nm had fallen to the lowest relative values and the irradiance from 1,000 to 1,100 nm was the highest. Nevertheless, at this depth in the mat the integrated irradiances over 100-nm ranges from 600 to 1,100 nm were quite comparable, spanning a total range from 22 to 53 μmol m^{-2} s^{-1}. These light conditions should be adequate to sustain all major groups of phototrophs at this depth. At a depth of 2 mm (Fig. 8C) the irradiance levels from 600 to 700 nm had fallen to less than 5 μmol m^{-2} s^{-1} (very low for cyanobacteria), whereas those above 800 nm ranged from 20 to 30 μmol m^{-2} s^{-1}. At 3 mm (Fig. 8D) the irradiances below 700 nm had fallen to very low levels (below 2 μmol m^{-2} s^{-1}), whereas those above 800 nm were still reasonable. These values continued to decrease, and at 5 to 6 mm (Fig. 8F and G) only the ranges of 900 to 1,000 nm and 1,000 to 1,100 nm exceeded 1 μmol m^{-2} s^{-1}.

DISCUSSION

Discussion of the method. The spectroradiometric techniques applied to field samples as described above provided a means of obtaining a rapid assessment of the spectral irradiance available in microbial mats as well as a rapid indication of the specific pigment-protein complexes present in the microorganisms making up the mat layers. The high wavelength resolution (readings were taken at 2-nm intervals), and subsequent sharpness of the troughs in the spectra due to absorption by pigments, permitted accurate identification of pigments and hence identification of the major groups of phototrophs present. This wavelength resolution was necessary to detect small pigment shoulders, to resolve pigments that absorb close to each other, and to detect low concentrations of pigments in situ against the complex background of the solar spectrum.

Although spectral irradiance values could be obtained by sectioning the mat and recording spectra through various thicknesses of the mat mounted over the irradiance sensor, use of the fiber-optic probe permitted measurements over smaller depth increments. The mat could not be sectioned well in less than 1-mm increments, whereas the probe could be advanced through the mat in increments of 100 μm. In practice, most of our measurements were made at 250- or 500-μm intervals. Use of the fiber-optic probe was much less destructive to the mat, and the sample could even be returned intact to the environment after spectral irradiance had been recorded.

The main limitation of the fiber-optic probes is that they are not irradiance sensors and only approximate the sprectral irradiance in situ. We have demonstrated that this is a reasonable approximation, however, and now have rough estimates of downward spectral irradiance in these mats. These approximations are best when measurements are made near solar noon in late spring and early summer. Jørgensen and Des Marais (9) have discussed the problems of measuring downward irradiance in mats with fiber-optic tips and have tried to measure downward irradiance and scalar irradiance by taking measurements at several angles and integrating the values over the hemisphere and sphere, respectively. In practice this is not only difficult but extremely time-consuming and not very practical for field studies such as ours. The best approach would be to develop a true irradiance sensor and preferably a spherical detector for measuring scalar irradiance directly. We have experimented with making spherical tips 1 mm or less in diameter but have not yet developed a true irradiance sensor. One such sensor has been described that uses an optical fiber inserted into a spherical diffuser (20), and the technical problems of developing irradiance and scalar irradiance sensors for use in microbial mats are probably surmountable.

Our present technique involves a totally portable field system suitable for approximating spectral irradiance in microbial mats at high wavelength resolution. The system is

TABLE 2. Upward irradiance as percentage of downward irradiance at selected wavelengths in plain wet sand and microbial mat at various depths

Depth (mm)	Upward irradiance[a] as % of downward irradiance at following wavelengths (nm):													
	370		436		676		748		844		1,016		350–1,100[b]	
	Sand	Mat	Sand	Mat	Sand	Mat	Sand	Mat	Sand	Mat	Sand	Mat	Sand	Mat
0.0	16.0	6.0	28.0	9.6	63.0	16.2	72.0	27.0	83.0	44.5	95.0	70.0	61.0	25.0
0.5	5.9	5.0	11.6	2.5	20.1	1.3	22.6	6.4	25.6	9.7	27.7	18.0	21.7	8.2
1.0	8.8	—	11.1	3.5	15.9	1.3	17.1	6.7	19.1	7.4	20.3	17.0	17.2	7.7
1.5	7.5	—	6.7	1.2	15.0	1.6	14.0	5.0	16.7	6.7	19.0	14.3	15.4	8.6
2.0	5.0	—	7.5	0.2	12.5	0	14.7	5.0	14.3	6.3	15.6	12.5	13.7	7.4
3.0	—	—	5.0	—	8.1	0	8.3	10.0	7.1	0	10.0	5.0	9.8	8.4
4.0	—	—	—	—	7.5	—	8.0	0	8.0	0	10.0	0	8.3	0

[a] —, Absence of value owing to lack of detectable downward and upward irradiance. A value of 0 was obtained when downward irradiance was detected but upward irradiance was not.

[b] The spectral irradiance was integrated over the range 350 to 1,100 nm before the percent upward irradiance was calculated.

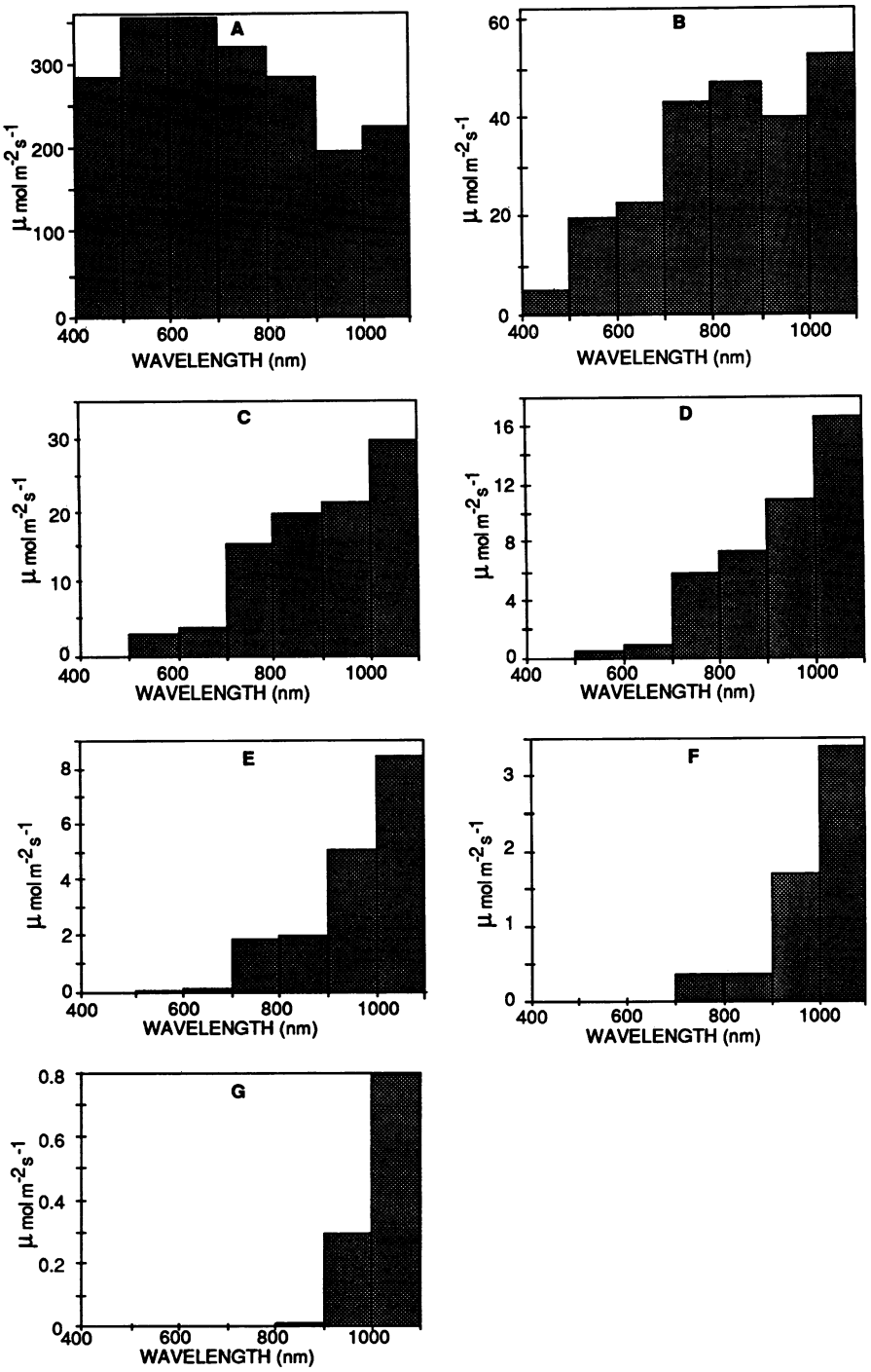

FIG. 8. Integrated spectral irradiance. The downward spectral irradiance at each depth in the mat was integrated over 100-nm intervals to better indicate the actual spectral irradiance available to sustain photosynthesis over the wavelength ranges absorbed by each pigment. (A) Surface; (B) 1.0 mm; (C) 2.0 mm; (D) 3.0 mm; (E) 4.0 mm; (F) 5.0 mm; (G) 6.0 mm.

rapid (20 min to set up completely; 20 min to record a mat profile). Depth resolution of 100 μm is possible, and the tips are very durable. We have analyzed well over 100 cores from a variety of mats and have never broken a tip. By making measurements at the field site on freshly collected cores, we have avoided transport problems and possible vertical migration of microorganisms during collection and storage. We believe that measurements of the light environment within the mat provide a more accurate description of prevailing conditions in the mat when they are made on mat cores freshly removed from the mat and use the natural solar light conditions prevailing at the field site where the mat is growing.

Distribution of spectral irradiance with depth and the effect of pigments. The spectral irradiance changed dramatically with depth in the mat at Great Sippewissett Salt Marsh. In

TABLE 3. Distribution of visible and NIR downward irradiance with depth

Depth (mm)	Irradiance (μmol/m²/s) (% of total irradiance at each depth)	
	400–700 nm	700–1,100 nm
0	996.0 (52.3)	909.0 (47.7)
1	47.3 (20.5)	183.0 (79.5)
2	7.6 (7.9)	88.0 (91.0)
3	1.6 (3.8)	41.0 (96.2)
4	0.2 (1.1)	18.0 (98.9)
5	0.1 (1.7)	5.9 (98.3)
6	0 (0)	1.1 (100.0)

general we saw that the blue end of the spectrum was most rapidly attenuated in the top layers of the mat, while the red and NIR radiation penetrated to greatest depths. Similar observations have been reported by others (3, 5–9). We have applied this analytical technique to several very different mats in hypersaline lagoons in Baja, Mexico, and in hot springs in Yellowstone National Park (B. Pierson, unpublished data). We can now make some generalizations about the penetration of radiation in phototrophic microbial communities. Owing to the presence of high levels of carotenoids in all surface-dwelling phototrophs, there is a strong attenuation of wavelengths from 400 to 550 nm. Further absorption in this region is due to the strong Soret bands of the chlorophylls (Chl *a* in the mat at Great Sippewissett) and to absorption by other pigments such as cytochromes and flavins present in all phototrophs. The combined effect of all of this absorption was nearly total attenuation (a reduction to 10^{-3} of surface irradiance values) of the spectrum from 400 to 550 nm within the top 2 mm of the mat surface. We have seen the same phenomenon in a wide variety of mats that we analyzed, including very thin, densely packed mats and thick, gelatinous, highly translucent mats. In most cases radiation below 550 nm was reduced to undetectable levels in the top 2 mm of the mat. When cyanobacteria form the surface layer, as at Sippewissett, absorption between 550 and 650 nm by the phycobilin accessory pigments attenuates radiation in this region and intense absorption by chlorophyll *a* at 670 nm strongly attenuates radiation in the region from 650 to 700 nm. Consequently, nearly all visible radiation from 400 to 700 nm is eliminated in the top 2 to 3 mm of such mats, leaving only NIR radiation available to sustain photosynthesis at greater depths. Table 3 illustrates this point by comparing the irradiance from 400 to 700 nm (commonly referred to as photosynthetically active radiation [PAR]) with the irradiance from 700 to 1,100 nm (NIR) at increasing depths in the Sippewissett mat. At the surface of the mat the energy of the incident solar radiation is nearly equal in these two ranges. Within the first 1 mm of the surface, however, selective attenuation at the lower wavelengths reduces the photosynthetically active radiation to 20% of the total irradiance. At 2 mm it is only 8% of the total and the NIR is more than 90% of the total irradiance. The significant "photosynthetically active radiation" below 3 mm is NIR, and the only photosynthetically active phototrophs at this depth are the purple and green photosynthetic bacteria. The significance of the NIR part of the solar spectrum for sustaining much of the ecosystem in microbial mat communities is now much clearer and can be specifically correlated with particular populations of phototrophs present in the communities.

The influence of specific chlorophyll pigments present in phototrophic microorganisms on the distribution of spectral irradiance with depth in the mat at Great Sippewissett Salt Marsh (Fig. 3, 4, and 6) was seen as very specific troughs in the spectra, despite the complex background of peaks and troughs (transmission minima) present in the incident solar spectrum. The location, wavelengths, and degree of attenuation by pigments in the microorganisms in the mat give a particular mat its own unique spectral signature when an irradiance depth profile is constructed (Fig. 6). Although most mats show a similar pattern of attenuation at the blue end of the spectrum, the unique spectral signature due to the presence of specific chlorophyll-protein complexes is revealed at the red end. Comparison of these signatures for different mats allows us to infer which organisms are present in the mats. For example, the signature of the Great Sippewissett mat (Fig. 6) is very different from the one obtained from a thick, gelatinous mat found in a thermal spring in Yellowstone National Park. This latter mat, near Rabbit Creek in the Midway Geyser Basin, was first described by Castenholz (2) and consists of an upper layer of cyanobacteria above a layer of *Chloroflexus aurantiacus* which, in turn, covers a layer of an undescribed filamentous bacterium containing an unusual Bchl *a* pigment-protein complex absorbing maximally at 804 and 915 nm (Pierson, unpublished). The distinct spectral signatures of these two different mats are most easily compared by using a single figure to display the entire depth range for each mat (Fig. 9). This can be done only when the logarithm of the irradiance is plotted, since the range in irradiance from the surface to the base of each mat is so great. The surface solar spectrum is very compressed on such a plot, but the signature of the mat is displayed well. Since the Bchl *a*-protein complexes absorb at such different wavelengths in the different bacteria present in these diverse mat environments, the troughs at 794 and 844 nm in the Great Sippewissett mat spectrum are absent in the Rabbit Creek Spouter mat spectrum and are replaced by troughs at 804 and 915 nm. This actually results in peaks in this spectrum near 790 and 840 nm. Since there are no Bchl *b*-containing bacteria in the thermal mat, there are no troughs in the spectra at 1,020 nm, in contrast with the spectrum of the Great Sippewissett mat.

Such light penetration signatures have now been obtained for a variety of mats (Pierson, unpublished), and the nature of the phototrophs making up the major communities within the mat can be identified quickly from these types of spectra. With both qualitative and quantitative effects on the light environments within the mat, the presence of a particular assemblage of phototrophs has a very profound influence on the spectral irradiance within the mat communities.

Characteristics of light penetration in the mat and in the plain sand matrix. The direct impact of pigmented microorganisms on the light environment within the mat was illustrated in Fig. 7. At the selected wavelengths in Fig. 7 (which corresponded to the absorption maxima of the chlorophyll pigments), penetration of radiation in the mat composed of pigmented phototrophs was greatly reduced over that in the plain sand. In some cases the difference in depth of penetration was several millimeters. This figure also illustrated, however, the very deep penetration of the red and NIR wavelengths in plain sand, which, as a matrix, was very transparent to these wavelengths. Even the blue wavelengths penetrated well to a depth of 5 mm (0.1% of surface irradiance). This observation is important in recognizing the possible significance of sediments, including sand, as a protective environment for the development of early phototrophs during the Precambrian era. Several millimeters of a sand matrix could significantly reduce the irradiance at the

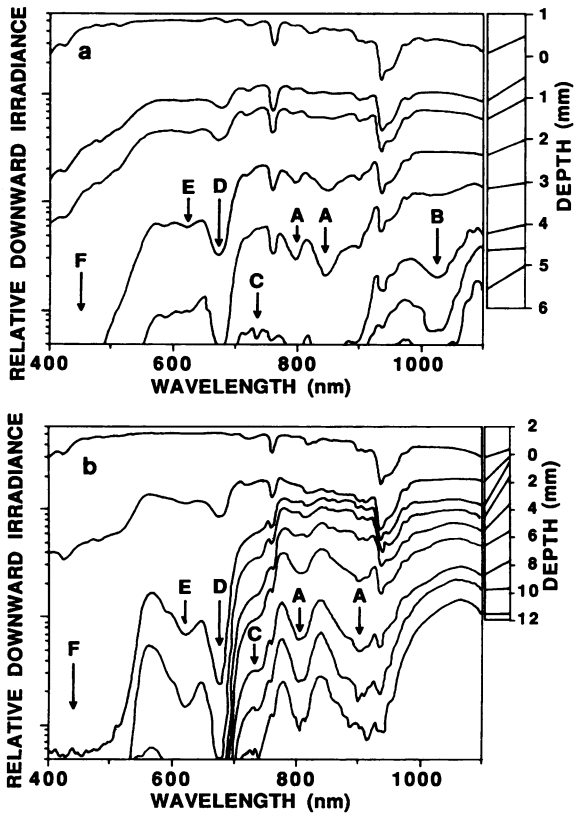

FIG. 9. Spectral irradiance signatures of two different mats. The relative downward spectral irradiance is plotted on a logarithmic scale as a function of depth in two very different mats: Great Sippewissett sand mat (a) and Rabbit Creek Spouter gelatinous mat from a thermal spring in Yellowstone National Park (b). Arrows indicate the minima in irradiance within the mat, caused by absorption by specific pigments occurring in each mat. Arrows: A, Bchl *a* absorbing at 794 and 844 nm in the Great Sippewissett mat and 804 and 910 nm in the Rabbit Creek Spouter mat; B, Bchl *b* absorbing at 1,015 nm in the Great Sippewissett mat and absent in the Rabbit Creek spouter mat; C, Bchl *c* absorbing at 748 nm in the Great Sippewissett mat and 740 nm in the Rabbit Creek Spouter mat; D, Chl *a* absorbing at 676 nm in both mats; E, phycocyanin absorbing at 622 nm in both mats; F, region of broad absorption by carotenoids in both mats.

damaging shorter wavelengths while transmitting sufficient irradiance in the red and NIR wavelengths to sustain primitive phototrophy.

Upward irradiance. Jørgensen et al. (5, 6, 9) noted the significance of upward or backscattered radiation in hypersaline mats from salt evaporation ponds. Near the surface (in the top few hundred micrometers) the upwelling or upward irradiance can be a very significant proportion of the light environment (9). We also found that in the very top of the Great Sippewissett mat, the upward irradiance had a major impact on the light environment seen by the cells (Table 2), although the proportion of upward irradiance was probably exaggerated by the error in our measuring system. Below 0.5 mm in the mat, however, the impact was much less significant. The percentage of backscattered radiation was greatest at longer wavelengths. At the longest wavelengths used by phototrophs (1,010 to 1,030 nm) the higher proportion of backscattered light could be significant, except that these organisms are found so deep within the mat (always below 3 mm) that they are in the range where upward irradiance has fallen to less than 5.0% of downward irradiance. The significance of upward irradiance for the anoxygenic phototrophs growing well below the surface of the Great Sippewissett mat does not appear to be very great. These organisms must depend primarily on downward irradiance. The cyanobacteria growing in the upper 0.5 mm, however, may obtain a significant portion of their photosynthetically active radiation from the upward irradiance. In plain sand, which lacks pigments to absorb radiation, the percent upward irradiance was much greater than in the mat at corresponding wavelengths and depths. The absorption of radiation by the phototrophs greatly reduced the availability of upward irradiance in this mat system.

TABLE 4. Distribution of total irradiance with depth

Depth (mm)	Irradiance (400–1,100 nm)	
	Amt (μmol $m^{-2}s^{-1}$)	% of surface irradiance
0	2,028	100.0
1	231	11.4
2	96	4.7
3	43	2.1
4	18	0.9
5	6	0.3
6	1	0.05

Irradiance available for different groups of phototrophs with depth. Several observations have been made on the sharp decrease in total irradiance that occurs with increasing depth in microbial mats (for example, see references 3 and 16). Although it is clear that the total energy available for photosynthesis drops sharply with depth in mats (Table 4), falling to values less than 1% of surface values at depths of 3 to 4 mm, studies such as those presented here and reported by others (3, 5–9) reveal that the spectral composition of this radiation is dramatically altered. In some cases the total amount of energy available may be adequate to sustain photosynthesis, but the specific wavelengths available may not be useful to some of the organisms at that depth. On the other hand, if organisms deep in the mat have the appropriate pigments, they may experience very low total irradiances that are highly enriched in the wavelengths absorbed by their pigments. To predict the possible occurrence of a particular phototroph at a given depth, one must know not only the irradiance at that depth but also its spectral composition.

The integrated values of spectral irradiance over 100-nm intervals presented in Fig. 8 are particularly useful because they give a better representation of the total radiation available to broadly absorbing pigment-protein complexes and those with closely spaced multiple peaks. From these data obtained at Great Sippewissett Salt Marsh, we can make some observations about the impact of total available irradiance on the distribution of various phototrophs with depth in this mat.

Below a depth of 3 mm, irradiance values were very low, yet most of the anoxygenic phototrophs were found at these depths. Below 3 mm only phototrophs capable of absorbing NIR wavelengths greater than 700 nm could possibly grow, and even these are likely to be severely limited by low irradiances. One interesting aspect of regarding the data in this manner is the revelation that although the NIR irradiances below 3 mm are sufficient to sustain the growth of phototrophs absorbing over ranges from 700 to 800 nm, 800

to 900 nm, 900 to 1,000 nm and 1,000 to 1,100 nm in this mat, organisms were not found that could utilize all of these wavelength ranges.

The purple sulfur bacteria containing Bchl *a*, absorbing from 800 to 900 nm, were found from 2.5 to 4.5 mm in this mat, and purple sulfur bacteria with Bchl *b*, absorbing from 1,000 to 1,050 nm, were found from 4 to 6 mm. Green sulfur bacteria with Bchl *c*, absorbing from 700 to 800 nm, were also found in this depth range. No organisms in this mat, however, absorbed radiation from 900 to 1,000 nm, although the irradiance in this range was similar to that in the other NIR ranges. That this radiation niche can be used has been verified by the presence of thin mats containing layers of *Chromatium tepidum* absorbing at 910 to 920 nm (11) and other very thick mats of filamentous Bchl *a*-containing phototrophs absorbing from 910 to 920 nm in hot springs in Yellowstone National Park (Fig. 9) (Pierson, unpublished). One might not expect there to be pigment-protein complexes absorbing over the entire 900- to 1,000-nm range merely because of the significant absorption by atmospheric water vapor in this range, resulting in a significant loss of solar irradiance at the Earth's surface from 920 to 960 nm. This loss is seen as the prominent trough in the solar spectrum over this range (Fig. 6A). However, on either side of this trough (from 900 to 920 and 960 to 1,000 nm) adequate radiation is available to sustain phototrophy. One might therefore expect to find organisms evolved to absorb this part of the NIR and might even expect them to exist deep in mats where these wavelengths can penetrate, as well as nearer the surface, where the irradiance is much greater. Such organisms were absent from the Sippewissett mats.

It appears that, indeed, all the anoxygenic phototrophs in the Great Sippewissett mat occurred in layers at depths exposed to NIR radiation absorbed by their bacteriochlorophylls. However, it is not clear why the sequence of their distribution was as observed. The irradiance at all NIR wavelengths found below 3 mm in the mat could sustain the anoxygenic phototrophs in any vertical sequence. The purple sulfur bacteria containing Bchl *b* could be located above the purple sulfur bacteria containing Bchl *a*, and both groups would still have adequate radiation to support photosynthesis (Fig. 8). The sequence of layers must therefore be determined by other environmental parameters such as oxygen and sulfide microzonation. It is well known that the Bchl *a*-containing phototrophs found in this mat are tolerant of oxygen and can even grow chemotrophically with oxygen under some circumstances. The fact that these phototrophs (*Chromatium* and *Thiocapsa* species) are found nearer the surface may be directly related to their oxygen tolerance, since this location puts them in direct contact with the layer of oxygenic cyanobacteria. The Bchl *b*-containing *T. pfennigii* is much less tolerant of oxygen, and its deeper location in the mat may reflect avoidance of oxygen. Likewise, the green sulfur bacteria are relatively intolerant of oxygen, and this may be significant in determining their deeper location in the mat. Experiments measuring photosynthetic activity of all three groups of anoxygenic phototrophs at Great Sippewissett (B. K. Pierson and J. Frederick, unpublished data) have confirmed that the deeper two groups are indeed light limited and would grow much better nearer the surface at the 3-mm depth if irradiance were the only factor to be considered. Their absence from these shallower depths is therefore due to some other factor such as inhibition by oxygen, limitation by lower sulfide levels, or competition for space and nutrients from the potentially faster-growing Bchl *a*-containing purple sulfur bacteria. The Bchl *b*-containing purple sulfur bacteria and the green sulfur bacteria grow at the greatest depths in the mat under severely radiation-limited conditions, apparently surviving only because they contain pigment-protein complexes that are able to absorb the limited wavelengths penetrating to these depths.

Significance of the penetration of radiation in sediments and mats for the evolution of pigment-protein complexes. The results of our studies on the penetration of radiation into mats and sediments have implications for understanding the early evolution of the diverse pigment-protein complexes found in the anoxygenic phototrophs. All of our data from the intertidal mats at Great Sippewissett Salt Marsh and from other mats show that the shorter wavelengths of the spectrum are attenuated very strongly in the upper 2 mm of mat and that only the red and NIR wavelengths penetrate deeper into the mat. Even in plain sand, it is the red and NIR wavelengths that penetrate the deepest. The anoxygenic phototrophs can grow near the surface and even at the surface of some mats when conditions are right, but usually cyanobacteria dominate the top 1 mm or more of mats and the anoxygenic phototrophs are found deeper. Owing to the limited wavelengths of light available at greater depths in mats, the anoxygenic phototrophs are the only organisms that can sustain phototrophy under these conditions. The far red and NIR absorption bands of their bacteriochlorophyll-protein complexes are essential for occupying this habitat (17). The tremendous diversity of the absorption bands in the protein complexes of Bchl *a*, Bchl *b*, Bchl *c*, Bchl *d*, Bchl *e*, and Bchl *g* permit the vertical layering of several different species using different parts of the red and NIR spectrum. In the Great Sippewissett mat, three different groups of anoxygenic phototrophs are able to use most of the NIR spectrum in this way. In mats in general, this diversity of NIR-absorbing pigment complexes confers an advantage on the various anoxygenic phototrophs, allowing them to compete successfully for the limiting resource of light to sustain phototrophy. The result is the formation of stratified communities, each layer of which uses and hence attenuates a specific part of the spectrum.

In aquatic environments, however, this diversity in NIR absorption properties of the Bchl-protein complexes confers little or no advantage to the anoxygenic phototrophs. The NIR wavelengths penetrate poorly in water and would be of use to sustain phototrophy in planktonic organisms only in extremely shallow environments. Figure 10 shows the spectral irradiance measured at the surface of a shallow hypersaline lagoon and the spectral irradiance at the surface of the mat below 50 cm of water. Even at this very shallow depth, there is little if any radiation beyond 900 nm, thus limiting the use of Bchl *a* and Bchl *b* complexes absorbing in this region. Although some radiation penetrates to this depth around 800 nm, which can be absorbed by most Bchl *a* complexes, there is little radiation at 840 to 900 nm, where most Bchl *a* complexes also absorb. The total availability of NIR radiation absorbed by Bchl *a* complexes is thus severely restricted in aquatic environments. Likewise, there is strong attenuation of radiation from 730 to 760 nm, where most of the light-harvesting Bchl complexes of the green bacteria absorb. In contrast, there is good penetration at this depth of radiation from 470 to 700 nm, the range in which the phycobilins, Chl *a* complexes, and carotenoids absorb. Although many anoxygenic phototrophs grow well as planktonic microorganisms deep in aquatic habitats (12, 13, 15), they must do so by using radiation of much shorter wavelengths absorbed by light-harvesting carotenoids and the Soret bands of their Bchl-protein complexes. It therefore

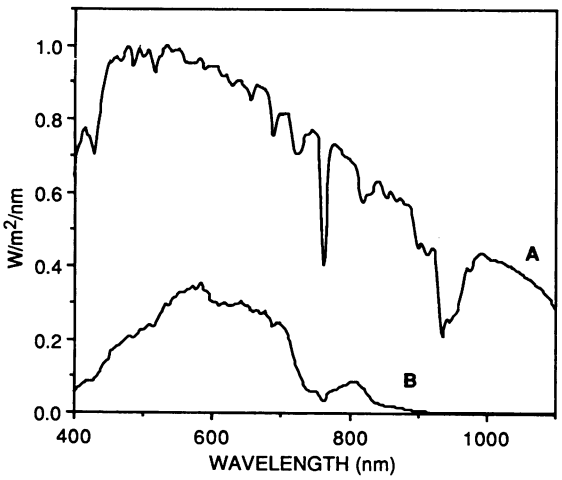

FIG. 10. Attenuation of NIR irradiance by water. Spectral irradiance at the surface of a hypersaline lagoon (A) and at the surface of a mat submerged 50 cm below the surface of the water (B).

seems most likely that the large diversity of Bchl-protein complexes found in the anoxygenic phototrophs evolved under conditions of growth in dense mat communities found in very shallow or surficial habitats (17). Under these conditions only, the presence of NIR-absorbing pigments would have been useful to the organisms and diversity would have conferred an advantage for survival when competing for light. Since most layers of individual groups of phototrophs that achieve thicknesses of 1 to 2 mm strongly attenuate the wavelengths absorbed by their pigments, diversity of pigment complexes is necessary if phototrophic mat communities develop to thicknesses much greater than this. It therefore seems likely that the early development of shallow, relatively thick phototrophic mats in the Precambrian era was preceded or accompanied by an early evolution of diverse pigment-protein complexes absorbing in the NIR in the anoxygenic phototrophs.

ACKNOWLEDGMENTS

This work was supported by National Science Foundation grant BSR-8521724 (RUI) and a Murdock Charitable Trust Grant from Research Corporation to B.K.P. Financial support as well as space and facilities for this research were provided to B.K.P. as an MBL Summer Research Fellow at the Marine Biological Laboratory, Woods Hole, Mass., during the summers of 1986 and 1987.

We thank David Nelson for assisting in making fiber-optic tips and for the design and construction of the micrometer table for field measurements. We thank Diane Holmstrom for technical assistance in the field, Bill Finley for developing the spectroradiometric data analysis system for the Macintosh computer, Scott Pierson for preparing the figures for publication, and Diane Blubaugh for assistance in preparation of the manuscript. We thank Li-Cor for assistance in determining the collecting properties of the fiber-optic tips. We thank the Salt Pond Areas Bird Sanctuaries, Inc., Falmouth, Mass., for permission to work in Great Sippewissett Salt Marsh.

LITERATURE CITED

1. **Bliss, D., and H. Smith.** 1985. Penetration of light into soil and its role in the control of seed germination. Plant Cell Environ. **8**:475–483.
2. **Castenholz, R. W.** 1984. Composition of hot spring microbial mats: a summary, p. 101–119. *In* Y. Cohen, R. W. Castenholz, and H. O. Halvorson (ed.), Microbial mats: stromatolites. Alan R. Liss, Inc., New York.
3. **Fenchel, T., and B. J. Straarup.** 1971. Vertical distribution of photosynthetic pigments and the penetration of light in marine sediments. Oikos **22**:172–182.
4. **Haardt, H., and G. Æ. Nielsen.** 1980. Attenuation measurements of monochromatic light in marine sediments. Oceanol. Acta **3**:333–338.
5. **Jørgensen, B. B.** 1989. Light penetration, absorption, and action spectra in cyanobacterial mats, p. 123–137. *In* Y. Cohen and E. Rosenberg (ed.), Microbial mats: physiological ecology of benthic microbial communities. American Society for Microbiology, Washington, D.C.
6. **Jørgensen, B. B., Y. Cohen, and D. J. Des Marais.** 1987. Photosynthetic action spectra and adaptation to spectral light distribution in a benthic cyanobacterial mat. Appl. Environ. Microbiol. **53**:879–886.
7. **Jørgensen, B. B., and D. J. Des Marais.** 1986. A simple fiber-optic microprobe for high resolution light measurements: application in marine sediment. Limnol. Oceanogr. **31**:1376–1383.
8. **Jørgensen, B. B., and D. J. Des Marais.** 1986. Competition for sulfide among colorless and purple sulfur bacteria in cyanobacterial mats. FEMS Microbiol. Ecol. **38**:179–186.
9. **Jørgensen, B. B., and D. J. Des Marais.** 1988. Optical properties of benthic photosynthetic communities: fiber-optic studies of cyanobacterial mats. Limnol. Oceanogr. **33**:99–113.
10. **Jørgensen, B. B., and D. C. Nelson.** 1988. Bacterial zonation, photosynthesis, and spectral light distribution in hot spring microbial mats of Iceland. Microb. Ecol. **16**:133–147.
11. **Madigan, M. T.** 1986. *Chromatium tepidum* sp. nov., a thermophilic photosynthetic bacterium of the family *Chromatiaceae*. Int. J. Syst. Bacteriol. **36**:222–227.
12. **Matheson, R., and R. Baulaigue.** 1977. Influence de la lumière solaire sur le développement des bactéries phototrophes sulfureuses dans les environnements marins. Can. J. Microbiol. **23**:267–270.
13. **Montesinos, E., R. Guerrero, C. Abella, and I. Esteve.** 1983. Ecology and physiology of the competition for light between *Chlorobium limicola* and *Chlorobium phaeobacteroides* in natural habitats. Appl. Environ. Microbiol. **46**:1007–1016.
14. **Nicholson, J. M., J. Stolz, and B. K. Pierson.** 1987. Structure of a microbial mat at Great Sippewissett Marsh, Cape Cod, Massachusetts. FEMS Microbiol. Ecol. **45**:343–364.
15. **Parkin, T. B., and T. D. Brock.** 1980. The effects of light quality on the growth of phototrophic bacteria in lakes. Arch. Microbiol. **125**:19–27.
16. **Pierson, B. K., A. Oesterle, and G. L. Murphy.** 1987. Pigments, light penetration and photosynthetic activity in the multilayered microbial mats of Great Sippewissett Salt Marsh, Massachusetts. FEMS Microbiol. Ecol. **45**:365–376.
17. **Pierson, B. K., and J. M. Olson.** 1989. Evolution of photosynthesis in anoxygenic photosynthetic procaryotes, p. 402–427. *In* Y. Cohen and E. Rosenberg (ed.), Microbial mats: physiological ecology of benthic microbial communities. American Society for Microbiology, Washington, D.C.
18. **Schubert, W., D. Giani, P. Rongen, W. E. Krumbein, and W. Schmidt.** 1980. Photoacoustic *in vivo* spectra of recent stromatolites. Naturwissenschaften **67**:129–132.
19. **Stal, L. J., H. van Gemerden, and W. E. Krumbein.** 1985. Structure and development of a benthic marine microbial mat. FEMS Microbiol. Ecol. **31**:111–125.
20. **Star, W. M., J. P. A. Marijnissen, and M. J. C. van Gemert.** 1987. Light dosimetry: status and prospects. J. Photochem. Photobiol. Ser. B **1**:149–167.
21. **Taylor, W. R.** 1964. Light and photosynthesis in intertidal benthic diatoms. Helgol. Wiss. Meeresunters. **10**:29–37.
22. **Taylor, W. R., and C. D. Gebelein.** 1966. Plant pigments and light penetration in intertidal sediments. Helgol. Wiss. Meeresunters. **13**:229–237.
23. **Tester, M., and C. Morris.** 1987. The penetration of light through soil. Plant Cell Environ. **10**:281–286.